Overcurrent Protection Coordination in a Power Distribution Network With the Active Superconductive Fault Current Limiter

Bin Li, *Member, IEEE*, Chao Li, Fengrui Guo, and Ying Xin, *Member, IEEE*

***Abstract*—The active saturated iron-core superconducting fault current limiter (SISFCL) is one of the best solutions to coping with high fault current levels and may be helpful in building future smart distribution networks. The application of an SISFCL in a distribution system can reduce the fault current to an acceptable level when a short-circuit fault occurs at different positions. The operational principle and the current-limiting characteristic of an active SISFCL are briefly introduced in this paper. The influence of an active SISFCL on the conventional inverse and definite time-delay overcurrent protective relays is discussed. In order to maintain reliable operation of the distribution system with an SISFCL, the protection coordination and setting solution is proposed. A model of a real 35-kV distribution system with an active SISFCL was built and simulated with the Electro-Magnetic Transients Program including DC software. Simulation tests have demonstrated the correctness and validity of theoretical analyses.**

***Index Terms*—Distribution systems, inverse time-delay, overcurrent protection, saturated iron core, superconductive fault current limiter (SFCL).**

I. Introduction

DUE TO the increases in power demand and high penetration of distributed generation, power distribution networks have been developed with the worldwide trend of smart grids [1]. However, the increasing fault current level is a troublesome challenge for secure and reliable operation of multi-source complex systems. Traditional current limiting solutions may lead to a permanent increase of the impedance not only at fault operation but also at normal power transmission. The latter is in conflict to the growing demand for a higher power quality and reducing power losses [2].

Superconductive fault current limiters (SFCLs) have been considered as a good solution to coping with large fault current [3]. An SISFCL was proposed in early 1980's for effective current limitation [4]. Since there is no superconductor quench required for the operation of an SISFCL, the cryogenic system of the device is simpler and costs less. Also, an SISFCL is able to provide large current limiting impedance, offering certain advantages. High temperature superconductor (HTS) was recommended to reduce the size and cost of an SISFCL [5]. By adding control logic to the dc magnetization circuit, an active SISFCL was proposed [6], [7]. Furthermore, a real SISFCL device with significant improvements in design was manufactured and installed in a distribution network for live grid operation [8]–[10]. Recently, the hybrid SFCL composed of a superconductor and a conventional limit reactor has been developed and installed in a distribution system. The operational performance of overcurrent relay and re-closer was demonstrated in this application [11], [12]. However, the settings coordination and sensitivity verification among the overcurrent protective relays of distribution systems with an active SISFCL have not been adequately addressed.

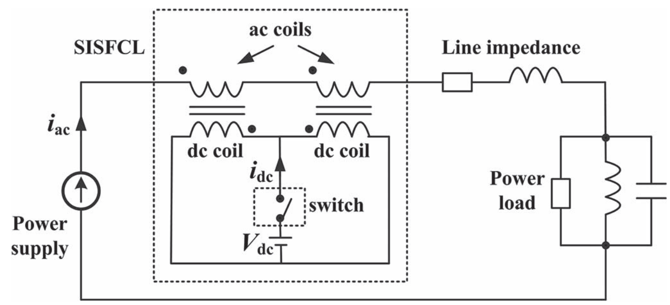

Fig. 1. Schematic electrical circuit of an SISFCL.

We carried out investigations of the inverse time-delay overcurrent protections and their coordination for a distribution network with the integration of an active SISFCL. The result is important in considering the reliable and secure operation of such a network.

II. Current Limiting Characteristics of an SISFCL

A typical SISFCL is composed of two iron cores, ac coils, and a superconductor dc coil with a magnetization circuit. The schematic circuit configuration diagram was shown in Fig. 1. The nonlinear impedance characteristic on the ac coils can be obtained by controlling the dc bias current passing through the dc superconductor circuit [3]–[7].

In order to solve some key technical problems, such as heavy weight, coupling problems between the ac and dc coils, and

Manuscript received May 8, 2014; accepted June 9, 2014. Date of publication July 1, 2014; date of current version July 11, 2014. This work was supported in part by the National Natural Science Foundation of China under Grant 51261130473, by the National High Technology Research and Development Program of China under Grant 2011AA05A106, and by the Program for New Century Excellent Talents in University of the Ministry of Education of China under Grant NCET-11-0367.

B. Li, C. Li, and F. Guo are with the Key Laboratory of Smart Grid of Ministry of Education, Tianjin University, Tianjin 300072, China (e-mail: binli@tju.edu.cn; lichao_tju@126.com; tjuguofengrui@126.com).

Y. Xin is with the Beijing Economic and Technological Development Area, Innopower Superconductor Cable Company Ltd., Beijing 100176, China (e-mail: yingxin@innopower.com).

Color versions of one or more of the figures in this paper are available online at http://ieeexplore.ieee.org.

Digital Object Identifier 10.1109/TASC.2014.2333811

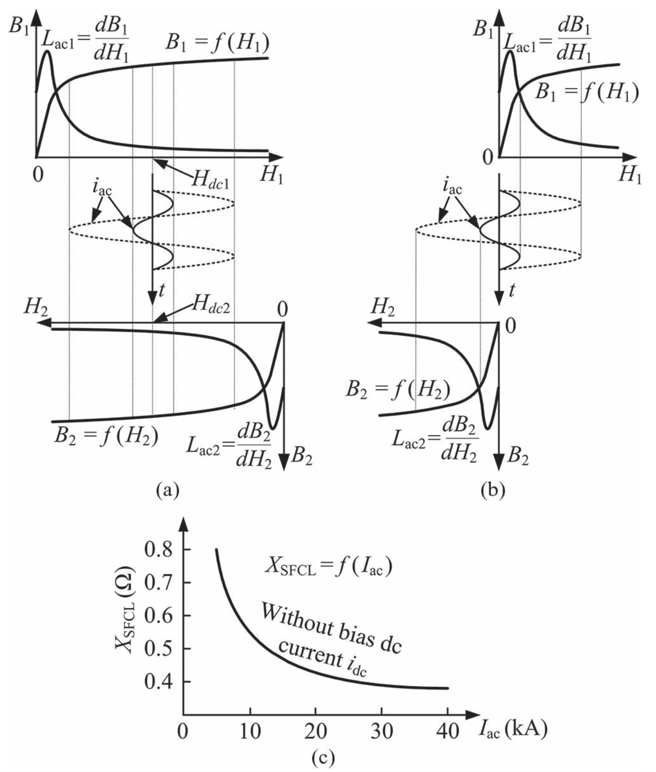

Fig. 2. Current limiting characteristics of SISFCLs. (a) passive SISFCL. (b) active SISFCL. (c) current limiting impedance of 35 kV SISFCL.

non-optimal limitation performance, specific iron-core structural design and a high-speed switch were introduced to realize a more efficient device, the so-called active SISFCL [7], [8]. In the normal power transmission condition, both iron cores are driven into deep saturation by the dc current $i_{\rm dc}$ which causes the magnetic circuits to operate around the dc bias magnetic fields $H_{\rm dc1}$ and $H_{\rm dc2}$ respectively. The inductances $L_{\rm ac1}$ and $L_{\rm ac2}$ are so small that the entire SISFCL is "invisible" to the power system, as shown in Fig. 2(a). In current limiting condition, both inductances $L_{\rm ac1}$ and $L_{\rm ac2}$ are very large because dc bias magnetic fields $H_{\rm dc1}$ and $H_{\rm dc2}$ are removed by switching off high-speed switch in the dc circuit, as shown in Fig. 2(b). Accordingly, the impedance characteristic of the active SISFCL is illustrated in Fig. 2(c). The impedance of the SISFCL is decreasing with the increasing of the fault current [13].

III. Coordination of Overcurrent Protection in a Distribution System With an SISFCL

A. *Inverse Time-Delay Overcurrent Protections and Their Coordination*

Fig. 3 shows a typical configuration of a power distribution system. As we know, the magnitude of the fault current decreases as the fault position moves away from the source. The inverse time-delay overcurrent relay is often used in distribution systems. Normal inverse time $t-I$ characteristic is used as an example in this paper, expressed as follows [14]:

$$t=\frac{0.14K}{(I_f/I_{act})^{0.02}-1} \tag{1}$$

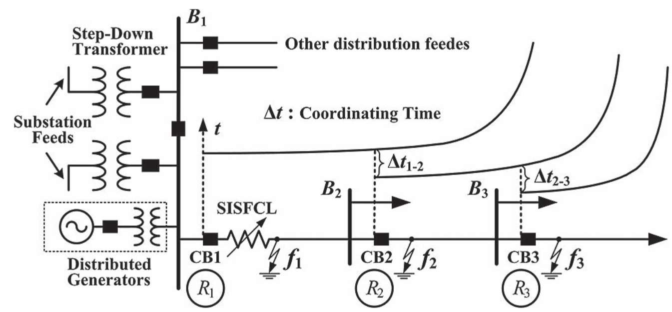

Fig. 3. Typical configuration of a power distribution system.

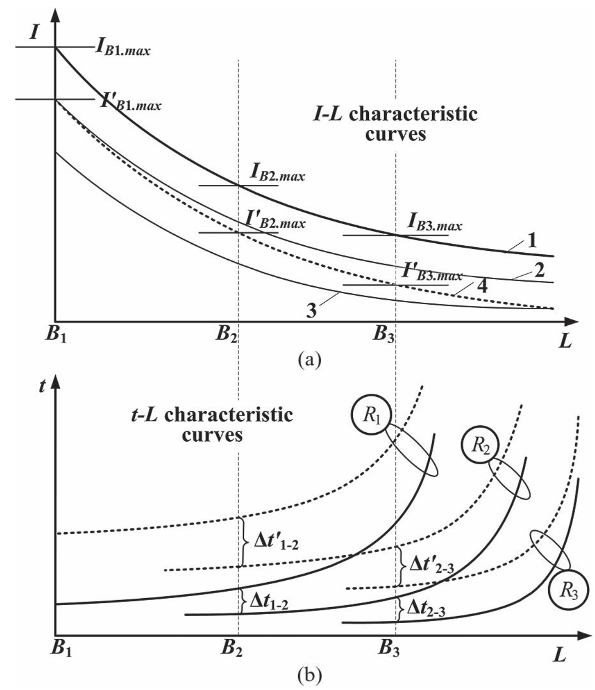

Fig. 4. Operation performance of inverse time-delay relay. (a) Fault current versus fault distance. (b) Operation time versus fault distance.

where I_f is the fault current, $I_{\rm act}$ is the pickup value as determined by the maximum load current, and K is the coefficient for adjusting the curve in vertical direction.

The principle of relay coordination can be explained as follows: for fault f_3 on the last section of the feeder, relay $\rm R_3$ operates first and breaker $\rm CB_3$ trips; relay $\rm R_2$ at breaker $\rm CB_2$ has a higher time lever setting that includes a coordinating time delay Δt_{2-3} (generally, $\Delta t \approx 0.3$ s–0.5 s) to allow breaker $\rm CB_2$ to trip if it can. Similarly, relay $\rm R_1$ coordinates with relay $\rm R_2$ by having a longer time delay Δt_{1-2}.

The relationship of fault current versus fault distance is illustrated in Fig. 4(a), where solid line 1 represents the feeder without SISFCL. It is assumed that the SISFCL is installed at the front part of the feeder. The current limiting effect of the SISFCL is different if the fault occurs at a different position. The farther the fault is, the larger the current limiting impedance is. For the distribution feeder with the SISFCL, the minimum and maximum impedances of the SISFCL are $X_{\rm min\,.SFCL}$ and $X_{\rm max\,.SFCL}$ respectively. In Fig. 4(a), solid lines 2 and 3 are with the constant current limiting impedances $X_{\rm min\,.SFCL}$ and $X_{\rm max\,.SFCL}$. Therefore, the characteristic of fault current through the feeder with the SISFCL is illustrated by the dashed line 4. Accordingly, the following essential conclusions can be obtained.

(1) The pickup value I_{act} of the inverse time-delay overcurrent is mainly determined by maximum load current. Therefore, it is not influenced by the SISFCL which is approximately "invisible" to power system in normal transmission condition.

(2) With the integration of the SISFCL, fault current level is decreased and the tripping time delay of each overcurrent relay is consequently lengthened, as shown by the dashed lines in Fig. 4(b). However, the coordination time interval between upstream and downstream protections is larger than the required value. In other words, the coordination among protections of the feeder is still maintained even if the original settings without considering the SISFCL are adopted

$$\begin{aligned}\Delta t'_{2-3} &= t'_{R2} - t'_{R3}\\ &= \frac{0.14K_{R2}}{(I'_{C.\max}/I_{act.R2})^{0.02}-1}\\ &\quad - \frac{0.14K_{R3}}{(I'_{C.\max}/I_{act.R3})^{0.02}-1}\\ &\succ t_{R2} - t_{R3} = \Delta t_{2-3}\end{aligned} \tag{2}$$

$$\Delta t'_{1-2} = t'_{R1} - t'_{R2} \succ \Delta t_{1-2}. \tag{3}$$

(3) It should be emphasized that the coordination between protection R_1 and upstream protection of the substation side must be verified. If the coordination time interval is not satisfied, the operating curves must be reset according to actual fault current curve 4 shown in Fig. 4(a).

(4) In field application, it is difficult for relay engineers to obtain curve 4. For simplicity, the relays can be reset according to solid line 2. In this way, not only is the coordination among the relays of the feeder and upstream substation side satisfied, but also the operation time delays are lengthened within a comparatively small scope.

B. Instantaneous and Definite Time-Delay Overcurrent Protection

For the inverse time-delay overcurrent protection, the closer the fault is to the source, the greater the fault current magnitude and the longer the tripping time. If the distributed feeder is comparatively long and there is substantial reduction of fault current as the fault is moved away from the source, the addition of instantaneous overcurrent relay will make the protection system viable. In order to ensure selectivity of the protection system, the pickup value of the instantaneous overcurrent protection must be set higher than the maximum fault current at the end of the local feeder. Since the fault current is decreased by applying the SISFCL on the feeder, the zone protected by the instantaneous overcurrent protection is reduced and the selectivity is guaranteed as well.

As opposed to the inverse time-delay overcurrent relay, the pickup value of the definite time-delay relay is not determined by the load current, but by the actual fault current. When the definite time-delay overcurrent relay is able to guarantee the sensitivity to the fault at the end the local feeder, its protecting zone may be beyond that of the downstream relay. This contradiction is much worse when the SISFCL is involved. Therefore, if the SISFCL is installed on the distribution feeder, the definite time-delay relays must be reset properly.

TABLE I
PARAMETERS OF THE SIMULATED DISTRIBUTION SYSTEM

Items	Value
System equivalent impedance	0.498 Ω
Distribution feeder	0.087 Ω / km
Maximum load of the feeder	50 MVA
Length of AB section	6 km
Length of BC section	5 km
Length of last section	2 km

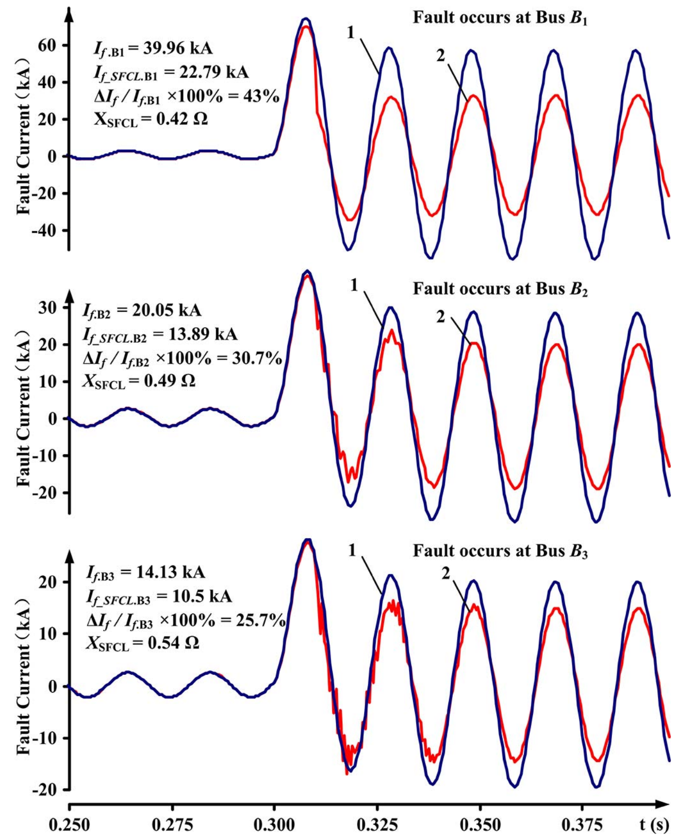

Fig. 5. Fault currents of three phase faults at buses B_1, B_2, and B_3.

IV. CASE STUDIES

A 35 kV distribution network with the protection system and the active SISFCL are simulated by EMTDC software based on the schematic in Fig. 3. The system parameters are listed in Table I.

Assuming a three phase short circuit fault takes place at buses B_1, B_2, and B_3 respectively, the fault current curves are shown in Fig. 5 where line 1 represents the cases without an SISFCL and line 2 represents the cases with an SISFCL. It can be clearly seen that the fault current is decreased significantly by applying the SISFCL.

With the integration of the SISFCL, it can be seen by comparing fault current values shown in Fig. 5 that the zone protected by the definite time-delay overcurrent relays will be beyond the downstream feeder in order to ensure enough sensitivity for the

TABLE II
OPERATION TIME DELAYS OF OVERCURRENT RELAYS IN THE CASES WITHOUT THE SISFCL

Inverse Time-delay Types	Fault point	Operation time of overcurrent relay		
		t_1	t_2	t_3
Normal Inverse Time-delay	f_1	0.488 s	-	-
	f_2	0.638 s	0.338 s	-
	f_3	0.755 s	0.400 s	0.100 s
Very Inverse Time-delay	f_1	0.271 s	-	-
	f_2	0.569 s	0.269 s	-
	f_3	0.846 s	0.400 s	0.100 s
Extreme Inverse Time-delay	f_1	0.124 s	-	-
	f_2	0.497 s	0.197 s	-
	f_3	1.010 s	0.400 s	0.100 s

TABLE III
OPERATION TIME DELAYS OF OVERCURRENT RELAYS IN THE CASES WITH THE SISFCL

Inverse Time-delay Types	Fault point	Operation time of overcurrent relay		
		t_1	t_2	t_3
Normal Inverse Time-delay	f_1	0.604 s	-	-
	f_2	0.762 s	0.404 s	-
	f_3	0.893 s	0.473 s	0.118 s
Very Inverse Time-delay	f_1	0.494 s	-	-
	f_2	0.864 s	0.408 s	-
	f_3	1.208 s	0.571 s	0.143 s
Extreme Inverse Time-delay	f_1	0.384 s	-	-
	f_2	1.046 s	0.414 s	-
	f_3	1.860 s	0.737 s	0.184 s

TABLE IV
COORDINATION TIMES AMONG INVERSE TIME-DELAY OVERCURRENT RELAYS ON THE FEEDER

Inverse Time-delay Types	Without SISFCL		With SISFCL	
	$\Delta t_{1\text{-}2}$	$\Delta t_{2\text{-}3}$	$\Delta t_{1\text{-}2}$	$\Delta t_{2\text{-}3}$
Normal Inverse Time	0.3 s	0.3 s	0.358 s	0.355 s
Very Inverse Time	0.3 s	0.3 s	0.455 s	0.428 s
Extreme Inverse Time	0.3 s	0.3 s	0.632 s	0.552 s

fault at the end of local feeder. Thus, its operation time has to be enlarged to ensure coordination.

If the normal inverse time $t - I$ characteristic is adopted in overcurrent relays on the feeder, the pickup values are assumed to be same for each relay, e.g., $I_{\text{act}} = 2$ kA. The coefficient K for each relay is set as $K_1 = 0.215$, $K_2 = 0.114$, and $K_3 = 0.029$. The operation time t_1, t_2, and t_3 of inverse time-delay overcurrent relays R_1, R_2, and R_3 on the feeder are determined by actual fault current and the operation (1). It is assumed that there is no SISFCL on the feeder at first. For the fault f_3, $t_3 = 0.1$ s and $t_2 = 0.4$ s, i.e. $\Delta t_{2-3} = 0.3$ s. Similarly, for the fault f_2, $t_2 = 0.338$ s and $t_1 = 0.638$ s, i.e. $\Delta t_{1-2} = 0.3$ s. The coordination among relays is guaranteed. Then the SISFCL is assumed to be installed on the feeder. For the fault f_3, $t_3 = 0.118$ s and $t_2 = 0.473$ s, i.e. $\Delta t_{2-3} = 0.355$ s > 0.3 s. For the fault f_2, $t_2 = 0.404$ s and $t_1 = 0.762$ s, i.e. $\Delta t_{1-2} = 0.358$ s > 0.3 s. Clearly, even though operation time delay is lengthened, the coordination among relays is still satisfied.

Numerous simulation tests have been carried out. Considering the cases with and without an SISFCL, Tables II and III provide operation time delays of overcurrent relays with different inverse time delay types. The coordination time intervals are calculated and displayed in Table IV.

For the distribution feeder with the active SISFCL, it is hard for definite time-delay overcurrent protection to have good coordination between speed and selectivity. Instead, it is recommended that the inverse time-delay overcurrent protection be used. It can operate within a comparatively short time-delay for the feeder faults, and the coordination of upstream and downstream protective relays is maintained.

V. CONCLUSION

An active SISFCL has prominent current limiting performance which is suitable for rapidly expanding distribution networks. According to its operational principle, the impedance of the SISFCL decreases with the increase of the fault current in the current limiting stage. The influence of the SISFCL on the inverse time-delay overcurrent protection system needs to be fully investigated. Our results demonstrate that the tripping time delay of each relay is lengthened due to the installation of the SISFCL. However, the coordination among inverse time-delay relays on the feeder is still guaranteed. Only the coordination among the relay of the upstream substation side and relays on the feeder with the SISFCL may need to be verified. For the definite time-delay overcurrent relay, the sensitivity and selectivity must be calculated based on the actual fault currents when an SISFCL is applied in the distribution feeder.

REFERENCES

[1] Y. Zhang and R. A. Dougal, "State of the art of fault current limiters and their applications in smart grid," in *Proc. IEEE Gen. Meet. Power Energy Soc.*, San Diego, CA, USA, Jul. 22–26, 2012, pp. 1–6.
[2] L. Ye, L. Lin, and K.-P. Juengst, "Application studies of superconducting fault current limiters in electric power systems," *IEEE Trans. Appl. Supercond.*, vol. 12, no. 1, pp. 900–903, Mar. 2002.
[3] M. Noe and M. Steurer, "High-temperature fault current limiters: Concepts, applications and development status," *Supercond. Sci. Technol.*, vol. 20, no. 3, pp. 15–29, Jan. 2007.
[4] B. P. Raju, K. C. Parton, and T. C. Bartram, "A current limiting device using superconducting d.c. bias applications and prospects," *IEEE Trans. Power App. Syst.*, vol. PAS-101, no. 9, pp. 3173–3177, Sep. 1982.
[5] J. X. Jin *et al.*, "Electrical application of high Tc superconducting saturable magnetic core fault current limiter," *IEEE Trans. Appl. Supercond.*, vol. 7, no. 2, pp. 1009–1012, Jun. 1997.
[6] V. Rozenshtein *et al.*, "Saturated cores FCL—A new approach," *IEEE Trans. Appl. Supercond.*, vol. 17, no. 2, pp. 1756–1759, Jun. 2007.
[7] Y. Xin, W. Z. Gong, and Z. J. Cao, "Development of saturated iron core HTS fault current limiters," *IEEE Trans. Appl. Supercond.*, vol. 17, no. 2, pp. 1760–1763, Jun. 2007.
[8] H. Hong *et al.*, "DC magnetization system for 35 kV/90 MVA superconducting saturated iron-core fault current limiter," *IEEE Trans. Appl. Supercond.*, vol. 19, no. 3, pp. 1851–1854, Jun. 2009.
[9] Y. Xin *et al.*, "Manufacturing and test of a 35 kV/90 MVA saturated iron-core type superconductive fault current limiter for live-grid operation," *IEEE Trans. Appl. Supercond.*, vol. 19, no. 3, pp. 1934–1937, Jun. 2009.
[10] Y. Xin *et al.*, "Saturated iron-core superconductive fault current limiter developed at Innopower," in *Proc. AIP Conf.*, 2014, vol. 1573, pp. 1042–1048.
[11] I.-K. You, S.-H. Lim, J. Kim, and O.-B. Hyun, "Study on protection coordination between protective devices in a power distribution system with an SFCL," *IEEE Trans. Appl. Supercond.*, vol. 20, no. 3, pp. 1168–1171, Jun. 2010.
[12] J.-S. Kim, S.-H. Lim, and J. Kim, "Study on application method of superconducting fault current limiter for protection coordination of protective devices in a power distribution system," *IEEE Trans. Appl. Supercond.*, vol. 22, no. 3, Jun. 2012, Art. No. 5601504.
[13] W. Z. Gong, J. Y. Zhang, T. Q. Wu, X. Y. Niu, and Y. Xin, "Current limiting characteristic of saturated iron core SFCLs," *J. Phys., Conf. Ser.*, vol. 234, no. 3, 2010, Art. No. 032016.
[14] S. E. Zocholl, J. K. Akamine, A. E. Hughes, and M. S. Sachdev, "Computer representation of overcurrent relay characteristics," *IEEE Trans. Power Del.*, vol. 4, no. 3, pp. 1659–1667, Jul. 1989.